

Numerical modelling of the underground roadways in coal mines– uncertainties caused by use of empirical-based downgrading methods and in situ stresses

M. Zoorabadi¹ and ²

1. Senior Geotechnical Engineer, SCT Operations, Wollongong, Australia

2. School of Mining Engineering, University of New South Wales, Sydney, Australia

Received 15 January 2018; received in revised form 21 February 2018; accepted 21 February 2018

Corresponding author: *m.zoorabadi@sct.gs; m.zoorabadi@unsw.edu.au (M. Zoorabadi).*

Abstract

Numerical modelling techniques are not new for mining industry and civil engineering projects anymore. These techniques have been widely used for rock engineering problems such as stability analysis and support design of roadways and tunnels, caving and subsidence prediction, and stability analysis of rock slopes. Despite the significant advancement in the computational mechanics and availability of high speed computing hardware, the input data and constitutive models remain the main source of errors affecting the reliability of numerical simulations. The problem with the input data has been deepened more by introducing empirical-based methods such as GSI classification to downgrade the rock properties from laboratory scale to field scale. The deformability modulus and strength parameters are the main outputs of these downgrading techniques. Numerical modelling users simply apply these downgrading methods and run the model without considering the real mechanics behind the stress induced failure and deformation around the underground excavations. While to the contrary to the commonly used downgrading methods that produce a constant modulus for rock at all depths, the rock modulus is stress dependent and varies with depth. In addition to this, the mechanism of stress induced displacement is not similar to the deformation of a continuum model simulated with equivalent rock properties. Apart from the mechanical characteristics of rocks, the magnitude and orientation of in-situ stresses are two other important parameters that have significant impacts on stress induced rock fracturing. The impacts of these two parameters have also been neglected in many practical cases. This paper discuss this old fashioned topic in more details with presenting the known facts and mechanics which numerical modelling users ignore them due to the unquestioning acceptance of downgrading methods. It also covers the influence of the stress magnitude and orientation on stress induced rock fracturing.

Keywords: *Numerical Modelling, Rock Failure, Empirical Methods, In Situ Stresses.*

1. Introduction

Underground excavations including roadways, panels, and stopes are means of access and extracting the underground reserves in mining industry. In addition, excavation of the underground structures is a common practice in civil engineering for infrastructure projects such as road tunnels, underground power plants, and underground storages. For all these cases, the underground excavations are created in rocks which their stability analysis and design impose a

number of different challenges to both civil and mining projects. Instabilities could cause a significant damage to the equipment, disruption to the operation/project or worse, fatalities with significant financial or social consequences.

Over the years, several methods have been introduced to assess stability of the underground excavations. All these methods can be classified into three main groups of empirical methods, numerical modelling methods and analytical

methods. Empirical methods forecast the rock behaviour and propose support system by comparing the geotechnical characteristics of the projects with historical dataset and experiences [1]. Although the reliability of these methods is in dispute, they are still common in both mining and civil engineering projects due to their simplicity to use.

Analytical methods use the fundamentals of the solid mechanics and provide formulations to calculate the stress distribution and the corresponding displacement around the excavations. Although these methods rely on too many assumptions and simplifications which limit their application for practical cases, they are brilliant for the initial analysis and understanding of the mechanics.

Numerical modelling methods are not new for both mining and civil engineering projects anymore. These methods have been applied for almost all these projects to assess the stability and to design the support system. Over the last two decades, several commercial software packages have been introduced to the industry. They have been developed on the basis of various numerical modelling techniques such as finite element, finite difference, distinct element, boundary element and combined methods [2]. The rapid advance in high speed computing hardware has also facilitated the use of numerical modelling in practice. Despite all these developments and acceptances, numerical modelling methods still suffer from an old fashioned problem that is the input data. In fact, the numerical modelling is absolutely a calculator that uses input data, conducts a series of mathematical operations, and gives outputs as the model results.

As a common practice, most numerical modelling users downgrade the rock mass strength and deformability data from laboratory results through empirical based methods. The GSI classification is the most well-known method for this downgrading approach [3]. It is very easy to use and it produces the required data very quickly. The users apply this method and build an equivalent continuum model and job done. The unquestioning acceptance of this approach results in just some well-presented and coloured graphs and pictures that in most cases do not match with the real behaviour of the underground structures. In addition to the strength and deformability characteristics, the magnitude and orientation of in-situ stresses are two other parameters that have significant impacts on the stress induced

fracturing and displacement of the underground excavation.

This paper discussed the mechanism of stress induced fracturing, and put insights into errors which are raised by blindly using of the rock strength and deformability downgrading techniques. It also shows how important is the stress magnitude and orientation for a reliable stability assessment of the underground excavation. The data from some real underground roadways in Australian coal mines were used to discuss the topic of the paper.

2. Instability modes for underground excavations

Instabilities in underground excavations can be classified in three groups: 1) structurally controlled instabilities caused by pre-existing discontinuities; 2) instabilities caused by stress induced rock fracturing; 3) combination of stress induced fracturing and pre-existing discontinuities [4].

Intersection of the pre-existing discontinuities forms blocks and they might fall or slide into the underground exaction when they have been cut by the excavation boundaries (Figure 1). Instability of the rock blocks is highly depended to their geometry and the frictional resistance of their forming surfaces [5]. For the blocks with sliding mode of movement, shear resistance on the sliding joints controls the stability. For all structurally controlled instabilities, stress around the excavation only has an impact on the frictional resistance of the joint surface. Since a larger size underground excavation provides a larger void for movement of the larger rock blocks, this type of instability should be assessed in more detail for larger excavations.

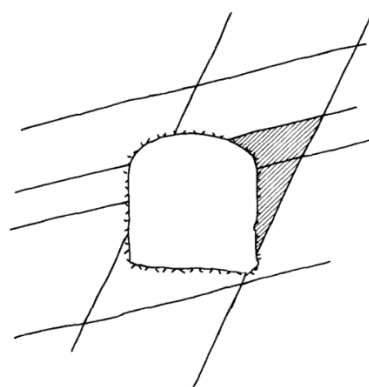


Figure 1. Rock blocks formed by intersection of pre-existing discontinuities and excavation boundaries [5].

The stress induced rock fracturing and associated displacements directly control the second and third types of instabilities. Underground excavations disturb equilibrium state of the in-situ stress and impose a new stress distribution [4]. Depending on the excavation geometry and in-situ stress tensor, magnitude of stress distribution (concentration) varies around the excavation. When magnitude of the new distributed stress exceeds the strength of the intact rocks (not rock mass), it causes rock fracturing.

The shear and extension (tensile) failure modes are two possible failure modes for a rock under triaxial and uniaxial loading conditions [6]. Both failure modes have been widely accepted by the industry and academics, and are included in all commercial numerical modelling software packages. The shear failure mode happens when the applied maximum principal stress exceeds the confined strength of the rock. On the basis of the Mohr-Coulomb failure criteria, the shear plane is oriented at an angle equal to $\pi/4 - \varphi/2$ with the orientation of σ_1 . For tension failure, the minimum principal stress is positive and is higher than the tensile strength of the rock.

Except for the rockburst event where a volume of rock fails in a violent way and breaks down to small pieces, rock fracturing occurs gradually as forming of a new fracture. Apart from the visible fracture plane, the rest of the rock volume also experiences micro-fracturing, which is not visible. This mechanism was observed in the laboratory scale like the triaxial tests [7]. At the end of the test, the macro-fracturing plane is visible as a shear plane. Micro-fracturing affects the deformability and strength (called softening in this paper) of the rock blocks in both sides of the failure plane (Figure 2).

The bearing capacity in the direction of failure plane is dropped to the residual strength of the failure plane. The plastic deformation of the softening zone due to its weight or because of acting stress is added to the initial elastic deformation which can be detected by a monitoring system.

Intersection of the stress induced rock fractures with the pre-existing discontinuities can form a removable block. The stability of these blocks again depends on their geometry relative to the excavation and the frictional resistance of their limiting surfaces.

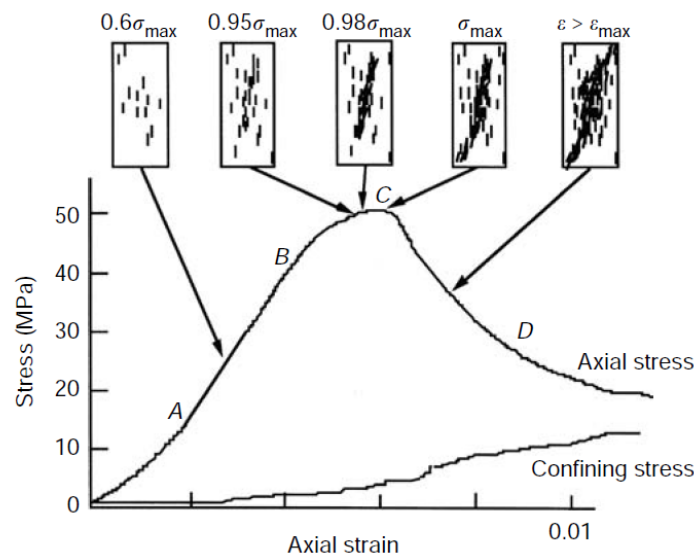


Figure 2. Micro-crack development and visible fracturing state observed in laboratory scale [7].

3. Uncertainties caused by use of downgrading methods

As mentioned earlier, rock strength and rock stress are the main parameters that control rock fracturing. Rock fails when the rock stress exceeds the rock strength. On the basis of the author's experience, for a cost effective 2D numerical modelling of an underground roadway in a coal mine (with a width of 5 m and a height

of 3 m), the element size is around 10 cm * 20 cm (rectangular zone size in FLAC2D). For a 3D model (FLAC3D) of the same roadway which takes at least 5-7 days to simulate 15 m length of the roadway, the element size is 10 cm * 20 cm * 25 cm. All the mesh based numerical modelling methods check the failure state of the individual zones for an elastic-plastic modelling (Figure 3). In fact, the software compares the strength of each

zone with the maximum stress acting on that zone. At the end of modelling, the software determines the failure zone around the roadway and corresponding displacements. Therefore, the final behaviour of the roadway is assessed by considering the failure mode and deformation of the individual zones as a whole system.

The following equation has been presented by [3] to calculate the downgrading ratio for the strength of the rock using the GSI classification:

$$\frac{\sigma_{cm}}{\sigma_{ci}} = \frac{(m_b + 4s - a(m_b - 8s)(m_b / 4 + s)^{a-1})}{2(1+a)(2+a)} \quad (1)$$

where σ_{cm} is the strength of rock mass, σ_{ci} is the strength of intact rock, and m_b , s , and a are constant parameters depending on the rock type and GSI value of the rock. The following equations are used to calculate the values of m_b , s , and a :

$$m_b = m_i \exp\left(\frac{GSI - 100}{28 - 14D}\right) \quad (2)$$

$$s = \exp\left(\frac{GSI - 100}{9 - 3D}\right) \quad (3)$$

$$a = \frac{1}{2} + \frac{1}{6}(e^{-GSI/15} - e^{-20/3}) \quad (4)$$

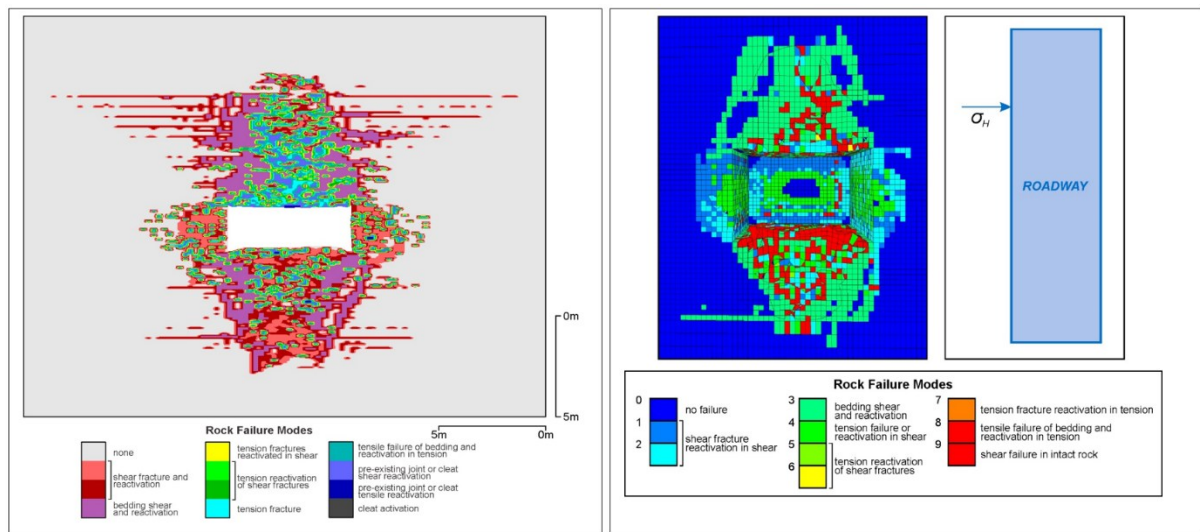


Figure 3. Failure modes around a coal mine roadway obtained using 2D and 3D modelling [8].

where, D is the disturbance factor which is estimated by using a provided descriptive classification; it is 0 for very well-controlled blasting practice and for mechanized excavation. m_i is the Hoek-Brown failure criteria constant for intact rock, which normally varies between 5 and 30 for different rocks.

For most of the coal measure rocks, there are three main pre-existing discontinuities including bedding planes, and two joint sets perpendicular to the bedding planes [9]. Therefore from the GSI classification methods, GSI value for a blocky rock mass formed by 3 or 4 joint sets varies from 50 to 70 for the surface quality of poor to good conditions (Figure 4). From Equation (1), for a rock mass with GSI values of 50-70 and $m_i = 17$ (typical value for sandstone) the downgrading ratio varies from 0.2 to 0.33. As seen in this figure, GSI-based downgrading method produces a downgrading ratio of 0.68 for a rock with GSI = 90. When GSI = 100 which presents an

absolute intact rock, the downgrading value is 1.2, which is an unacceptable value.

When this downgrading method is applied to a numerical model, it is assumed that all the numerical model zones have same GSI values. For coal measure rocks, this assumption means that all numerical zones have at least 3 discontinuity sets. This is a very conservative assumption (Figure 5). For typical Bulli seam coal measure rocks (located in Illawarra colliery, NSW Australia), a downgrading ratio of 0.25 was applied to the UCS of the strata surrounding a roadways located 500 m below the ground surface. The 3D numerical modelling of this roadway gives a very unreliable displacement that interrupted the simulation process and the model could not run further (Figure 6). This modelled behaviour is completely different from the monitored behaviour of the typical roadways during development. This example simply shows that the downgrading ratio unreliably reduces the strength of the coal measures rocks and thus is not acceptable.

In addition to the strength of the rocks, downgrading methods for deformability modulus also imposes a big uncertainty to the numerical modelling. Over the years, too many empirical equations have been introduced by researchers

and engineers by correlating the field measurements with well-known classification systems such as RMR, Q, GSI, and R_{Mi}, Shen et al., (2012) [10] listed these equations as Table 1





<p>GEOLOGICAL STRENGTH INDEX</p> <p>From the letter codes describing the structure and surface conditions of the rock mass (from Table 4), pick the appropriate box in this chart. Estimate the average value of the Geological Strength Index (GSI) from the contours. Do not attempt to be too precise. Quoting a range of GSI from 36 to 42 is more realistic than stating that GSI = 38.</p>		<p>SURFACE CONDITIONS</p> <p>VERY GOOD Very rough, fresh unweathered surfaces</p> <p>GOOD Rough, slightly weathered, iron stained surfaces</p> <p>FAIR Smooth, moderately weathered or altered surfaces</p> <p>POOR Slickensided, highly weathered surfaces with compact coatings or fillings of angular fragments</p> <p>VERY POOR Slickensided, highly weathered surfaces with soft clay coatings or fillings</p>				
<p>STRUCTURE</p>		<p>DECREASING SURFACE QUALITY ➤</p>				
<p>DECREASING INTERLOCKING OF ROCK PIECES ➤</p>	 <p>BLOCKY - very well interlocked undisturbed rock mass consisting of cubical blocks formed by three orthogonal discontinuity sets</p>	80	70	60	50	40
	 <p>VERY BLOCKY - interlocked, partially disturbed rock mass with multifaceted angular blocks formed by four or more discontinuity sets</p>					
	 <p>BLOCKY/DISTURBED - folded and/or faulted with angular blocks formed by many intersecting discontinuity sets</p>					
	 <p>DISINTEGRATED - poorly interlocked, heavily broken rock mass with a mixture of angular and rounded rock pieces</p>					
					30	20
						10

Figure 4. Typical GSI table [3].

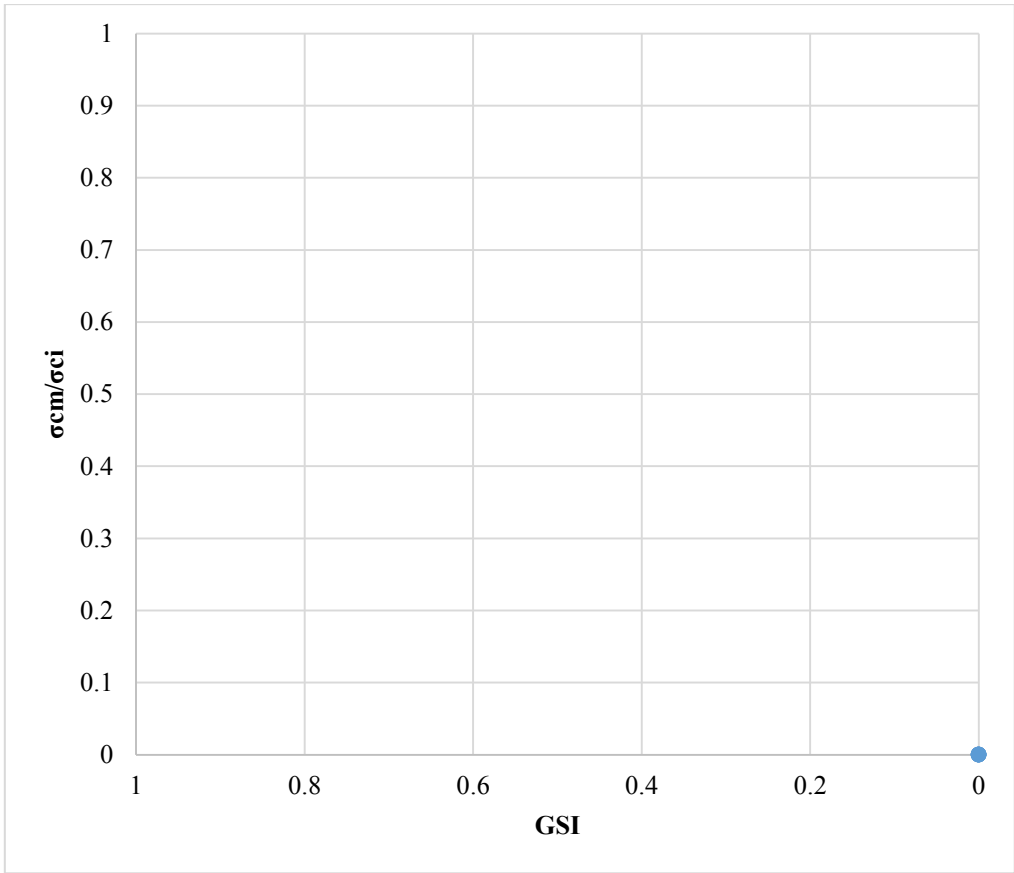


Figure 5. Downgrading ratio on basis of GSI classification.

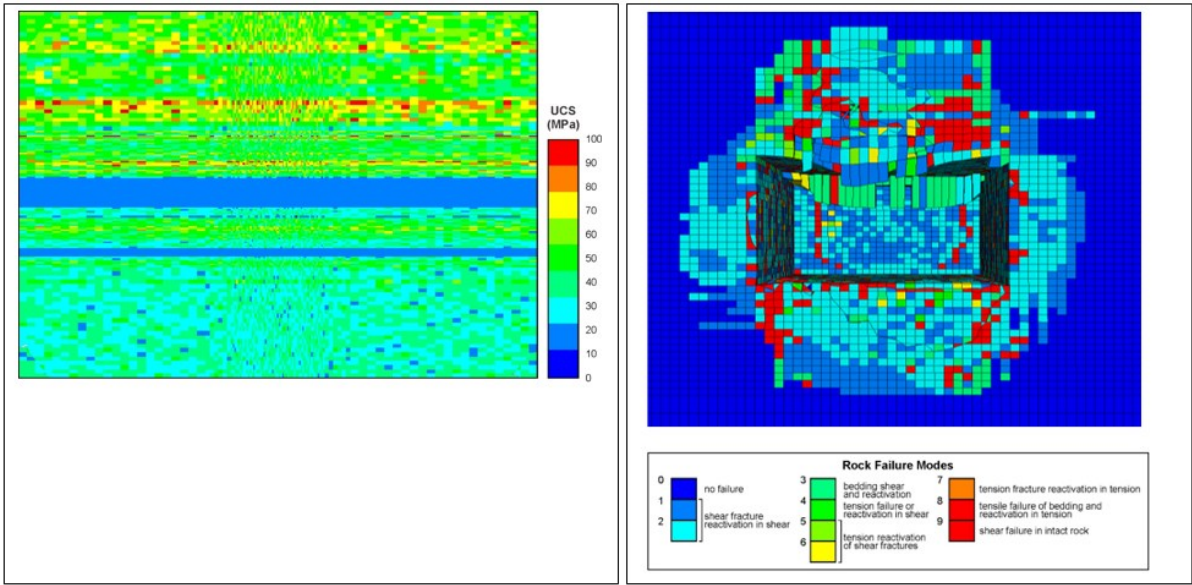


Figure 6. UCS variation of typical Bulli seam coal measure rocks and failure modes for downgrading ratio of 0.25.

Table 1. Empirical equations using RMR and GSI [10].

Input parameters	Empirical equations	
Group 1 RMR	Bieniawski (1978)	$E_m = 2RMR - 100, RMR > 50$
	Serafim and Pereira (1983)	$E_m = 10^{(RMR-10)/40}$
	Mehrotra (1992)	$E_m = 10^{(RMR-20)/38}$
	Read et al. (1999)	$E_m = 0.1(RMR / 10)^3$
Group 2 RMR and E_i	Nicholson and Bieniawski (1990)	$E_m = 0.01E_i(0.0028RMR^2 + 0.9e^{\frac{RMR}{22.83}})$
	Mitri et al. (1994)	$E_m = E_i[0.5(1 - (\cos(\pi RMR / 100)))]$
	Sonmez et al. (2006)	$E_m = E_i 10^{((RMR-100)(100-RMR))/(4000 \exp(-RMR/100))}$
Group 3 GSI and D	Hoek et al. (2002)	$E_m = (1 - 0.5D)10^{\frac{(GSI-10)}{40}}, \sigma_{ci} > 100 \text{ MPa}$
	Hoek and Diederichs (2006)	$E_m (\text{MPa}) = 10^5 \left(\frac{1 - 0.5D}{1 + e^{(75+25D-GSI)/11}} \right)$
Group 4 GSI, D and E_i	Carvalho (2004)	$E_m = E_i(s)^{0.25}, s = \exp\left(\frac{GSI - 100}{9 - 3D}\right)$
	Sonmez et al. (2004)	$E_m = E_i(s^a)^{0.4}, s = \exp\left(\frac{GSI - 100}{9 - 3D}\right), a = 0.5 + \frac{1}{6}(e^{-GSI/15} - e^{-20/3})$
	Hoek and Diederichs (2006)	$E_m = E_i(0.02 + \frac{1 - 0.5D}{1 + e^{((60+15D-GSI)/11)}})$
Group 5 GSI, D and σ_{ci}	Hoek and Brown (1997)	$E_m = \sqrt{\frac{\sigma_{ci}}{100}} 10^{\frac{(GSI-10)}{40}}$
	Hoek et al. (2002)	$E_m = (1 - 0.5D) \sqrt{\frac{\sigma_{ci}}{100}} 10^{\frac{(GSI-10)}{40}}, \sigma_{ci} \leq 100 \text{ MPa}$
	Beiki et al. (2010)	$E_m = \tan\left(\sqrt{1.56 + (\ln(GSI))^2}\right) \sqrt[3]{\sigma_{ci}}$

Deformability of the jointed rocks is controlled by deformation of the intact rock blocks and pre-existing discontinuities [3]. Zoorabadi (2010), [11], performed a parameter study on some of the existing empirical equations to explore the contribution of the intact rock and the rock mass condition to the deformability modulus estimated from those equations. It was found that in the Hoek and Brown (1997)'s equation, intact rock properties (UCS) had small contribution to the rock mass modulus. This condition was modified in the Hoek and Diederichs (2006)'s equation (most common equation in practise) which considers more contribution for the intact rock property (Figures 7a, b).

Stress dependency of the deformability modulus that was not considered in the empirical equation is the main shortcoming of all these equations. Deformability of the rock discontinuities and rotation of the rock block have significant influences on the deformability of the jointed rocks located at ground surface, where the stress level is negligible.

A normal stress applied on a rock fracture causes the fracture to close and decreases the aperture. Goodman (1989), [4], performed laboratory tests

and found a significant nonlinear relationship between the applied stress and the fracture closure. He also found that the nonlinear trend approaches an asymptote at high stress values. Therefore, deformability of the rock mass containing discontinuities would have different values at different depth or stress level.

Zoorabadi (2016), [12] applied the analytical formulation proposed by Li (2002) and developed an approach to assess the variation in the deformability modulus at different depths. This technique was applied to a real case where the rock mass including 4 pre-existing discontinuities. The elastic modulus obtained from laboratory tests for the intact rock was 16 GPa. The GSI value for the rock mass estimated from the available geological information varied between 60 and 70 with an average of 65. For this average GSI value, the deformability modulus calculated using the equations proposed by Hoek and Diederichs (2006) is approximately 10 GPa.

The variation in the deformability modulus with depth calculated by the approach proposed by [12] is shown in Figure 8. This figure shows that the deformability modulus of this case at the ground surface (zero acting normal stress was assumed) is

approximately 7.2 GPa. This value is around 0.45% of the elastic modulus of the intact rock and demonstrates the controlling contribution of the discontinuity to the deformability of the block. Deformability modulus of the rock mass block increases significantly with increase in depth. As it can be seen, just at the 50 m depth, it would have a magnitude of 12.5 GPa which is 0.78% of

the elastic modulus of the intact rock. For depths deeper than 200 m, the deformability modulus of the rock mass block would be more than 90% of the elastic modulus of the intact rock. These results highlight a decreasing trend for the contribution of the pre-existing discontinuities to deformability of the jointed rocks when depth increases.

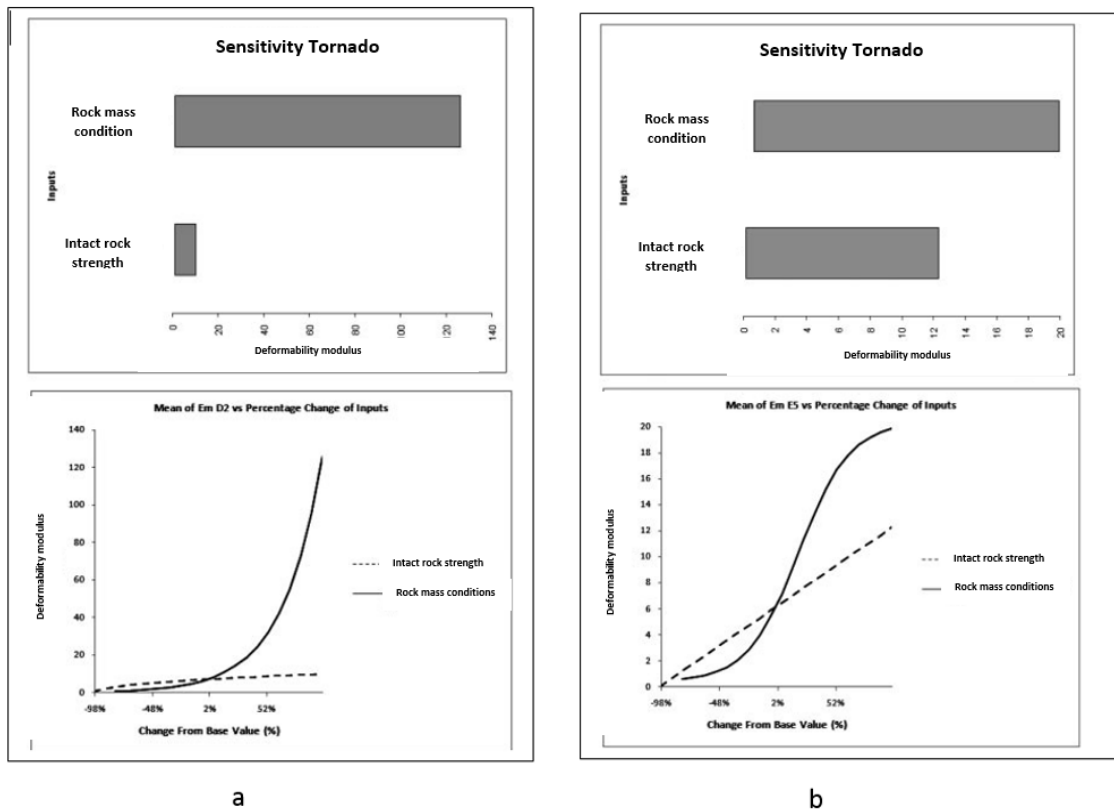


Figure 7. Parameter study on empirical-based deformability modulus equations [11].

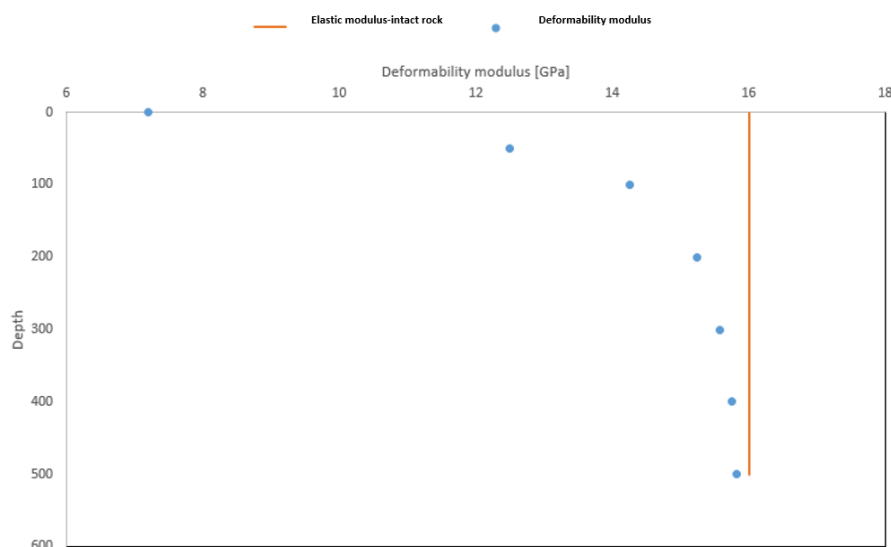


Figure 8. Variation of deformability modulus with depth [12].

4. Uncertainties caused by stress magnitude and orientation

In situ stress tensor acting on a rock at depth consists of one vertical component and two horizontal components (Figure 9). The vertical stress is generated by the overburden strata weight and increases proportional to the depth. It is expected that the overburden load increases 2.2 - 2.5 MPa per 100 m depth [13].

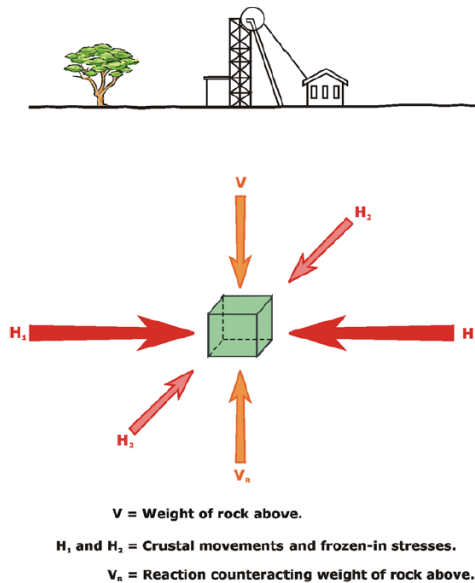


Figure 9. Stress acting on rock at depth [9].

The horizontal stress components are generated due to two source of reactions one from overburden stress (σ_{H-G}) and the other from the tectonic forces (σ_{H-T}) as follows [14]:

$$\sigma_H = \sigma_{H-G} + \sigma_{H-T} \quad (5)$$

The horizontal stress generated as a reaction to the overburden stress comes from the lateral movement and the Poisson impact. Magnitude of the Poisson reaction to the overburden stress is calculated as follows:

$$\sigma_{H-G} = \frac{\nu}{1-\nu} \sigma_V \quad (6)$$

where ν is the Poisson ratio for rock. For a Poisson ratio of 0.25, the overburden contribution to the horizontal stress is approximately $\frac{1}{3} \sigma_V$.

The lateral movement of the continental plates forming the Earth's crust is another main source for the horizontal stress components. The continental drift, which is monitored by the satellite global positioning system, moves the continents at a few centimetres per year, causing collisions and shearing along the continental

boundaries [15]. This movement acts as a force applied to the Earth's crust that increases the horizontal stresses.

As a common practice for the numerical modelling, a constant ratio between the horizontal stress and the vertical stress is used to initialise the in situ stresses for the whole model. Additionally, since the 2D model is easier and cost effective, the impact of stress orientation on the numerical modelling is ignored in practice.

When an underground excavation is constructed in a geological domain with the same elastic modulus, the assumption for a constant stress ratio is reasonable. However for a stratified ground such as coal measure rocks where the elastic modulus of the strata varies significantly, this assumption causes a significant error for numerical modelling.

The tectonic force generated by continental plate movement is applied as a force to the Earth's crust. When the crust is formed from material units with different elastic modulus, the horizontal stress developed in each unit would be different. This concept was well presented by [14], as in Figure 10. Based on this concept, the horizontal stress magnitude is typically proportional to the stiffness of the material in which the measurement was taken. The horizontal stress in softer strata is lower than the stress in the stiffer units. The minimum horizontal stress is also affected by material stiffness whose direction is 90 degree to the maximum horizontal stress.

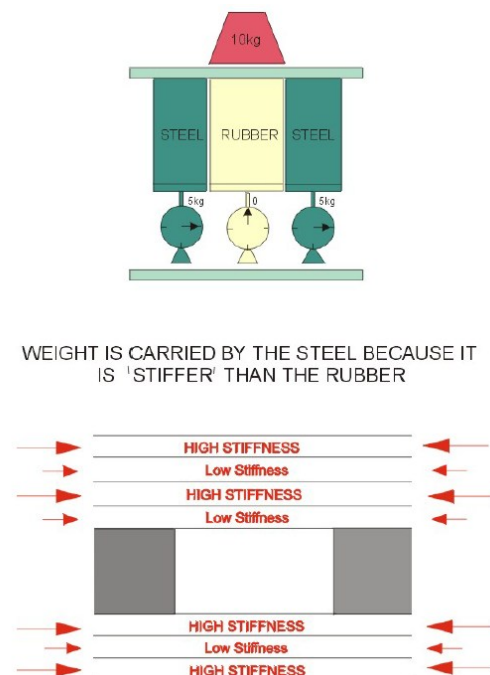


Figure 10. Concept of variation of horizontal stress developed in different layers [14].

The magnitude of the horizontal stress for each rock unit is calculated using the following formulation [14]:

$$\sigma_H = \left(\frac{\nu}{1-\nu}\right)\sigma_v + E \times TSF \quad (7)$$

where σ_H is the total horizontal stress (MPa), σ_v is the vertical stress (MPa), ν is the Poisson ratio, E is the Young's modulus (GPa) and TSF is the tectonic stress factor. The measured range for the tectonic stress factor from Australian coal mines is presented in Figure 11 [14].

Therefore for the coal measure rocks, the horizontal stress developed in coal with elastic modulus of 2-4 GPa is much less than the horizontal stress in the stiffer roof or floor strata. This is the main reason for why a coal roof is designed for the roadways in thick seams. For Bulli seam geology in Australia the maximum horizontal stress distribution for a tectonic stress of 1.4 would be as Figure 12. The maximum horizontal stress in coal seam is approximately 7.5 MPa while the stress in the stiffer unit reaches up to 38 MPa.

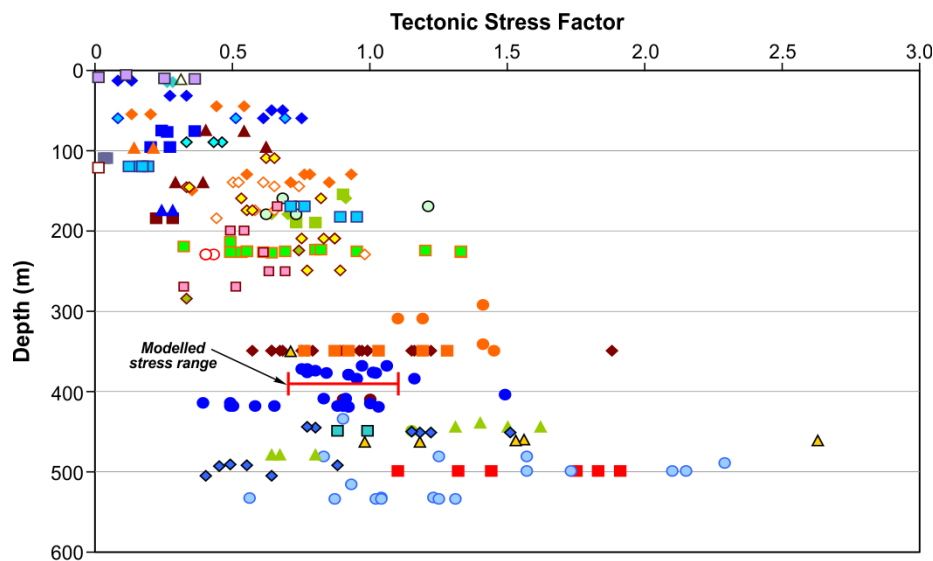


Figure 11. Tectonic stress factor vs depth for Australian coal mines.

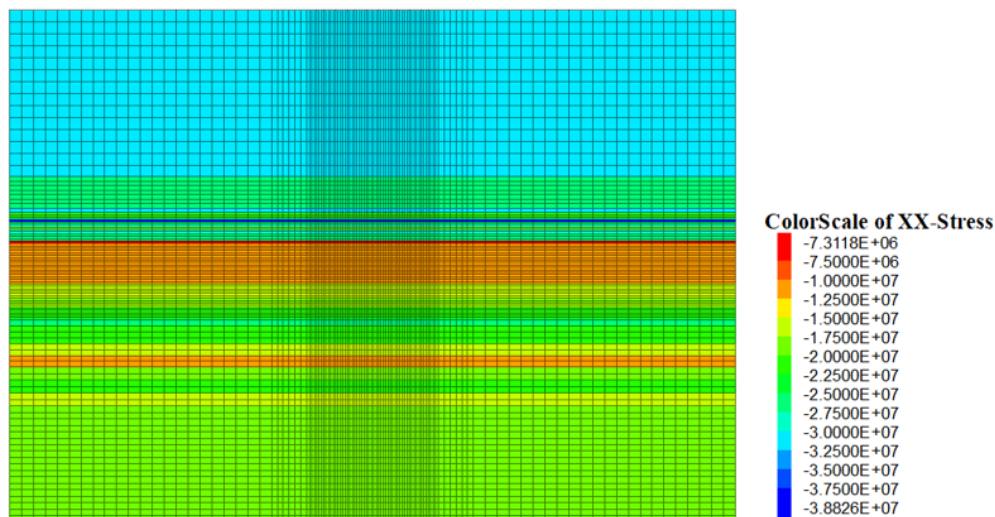


Figure 12. Horizontal stress developed in typical Bulli seam conditions.

The stress orientation impact on the numerical modelling of the underground excavations is also vital but it is neglected in practice due to 2D modelling. The horizontal stresses has two components as maximum and minimum stresses. These two components and their orientation plays

a big role on the stress induced fracturing around the underground excavations. Gale and Blackwood (1986) simulated the impact of the stress orientation on the stress concentration around the roadways in coal mines [16]. They showed that the stress concentration is a function

of stress orientation. A summary of stress monitoring results from a range of longwall panels is presented in Figure 13, which shows the stress concentration relative to the angle of stress to the main gate. The stress concentrations tend to maximise in the 40-70° range.

Zoorabadi and Rajabi (2017) used 3D numerical modelling to assess the impact of the bedding plane on the softening zones forming around the roadways in coal mines [17]. They show that the stress orientation is one of the main controlling parameters for type and extension of failure zones in bedded and laminated strata (Figure 14).

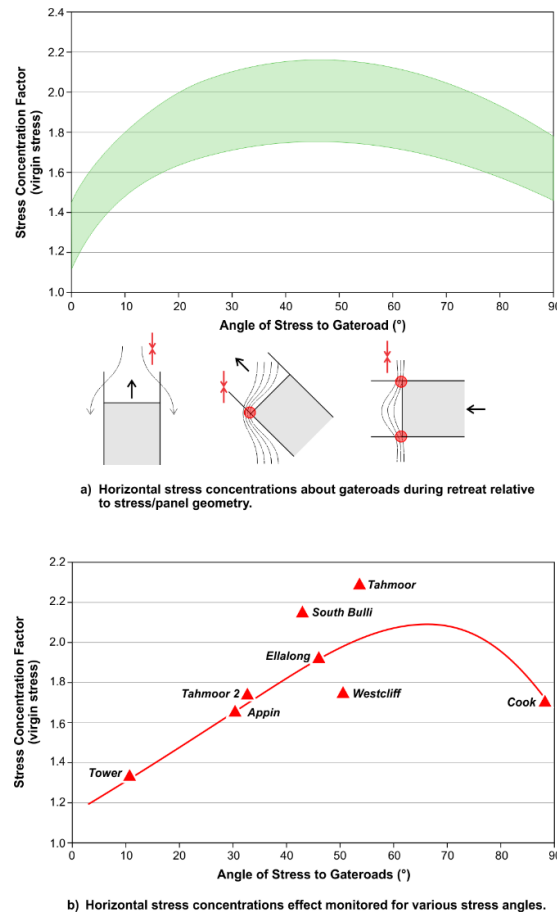


Figure 13. Stress concentration around the roadway for various stress orientation relative to roadway [18].

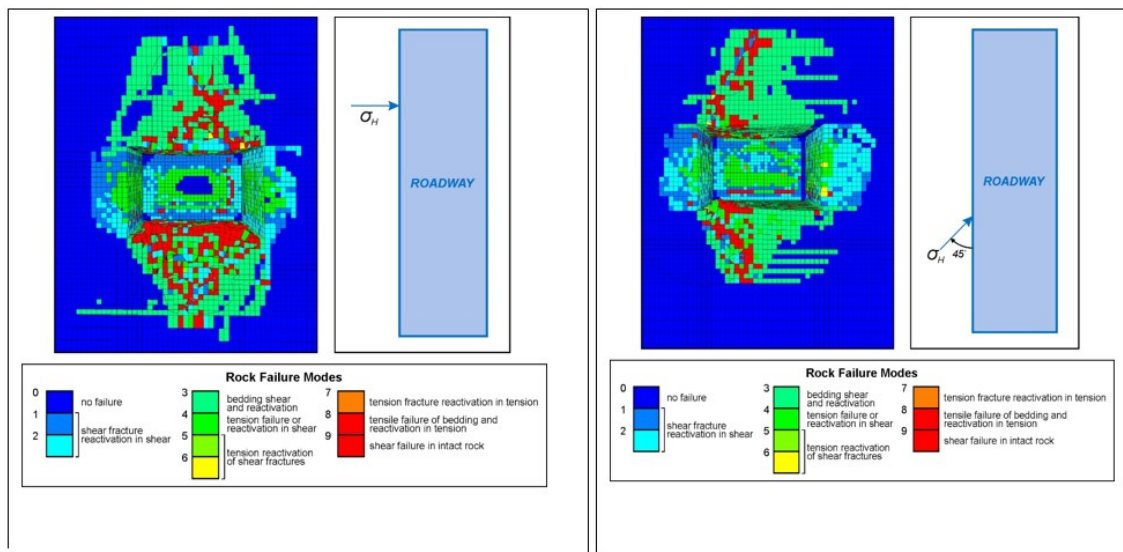


Figure 14. Impact of stress orientation on type and extension of failure zones in stratified rock around roadways [17].

5. Conclusions

Numerical modelling is commonly used for analysing underground excavations in both the civil and mining engineering projects. This method applies various computational methods to the input data provided by the user and produces results in the forms stress, strain, and failure modes. As a common practice, downgrading methods based on rock classification systems have been used to estimate the strength and deformability characteristics of rocks. This paper showed how using these downgrading methods can cause a considerable uncertainty for stability assessment of underground roadways in coal mines. Additionally, the magnitude and orientation of in situ stress have a significant impact on the results of numerical methods. It was shown that applying a constant stress ratio to stratified rocks such as coal measure rocks is not representing the real stress field. The 3D modelling is vital for a reliable assessment of the stress orientation impact on the roadway behaviour. The failure modes and extension are both controlled by stress orientation in coal measure rocks.

References

- [1]. Palmström, A. (1995). RMI- A Rock Mass Characterisation System for Rock Engineering Purposes. University of Oslo. Norway.
- [2]. Jing, L. and Hudson, J.A. (2002). Numerical methods in rock mechanics. *Int. J. Rock Mechanics and Mining Science*. 34: 409-427.
- [3]. Hoek, E. and Brown, E.T. (1997). Practical estimates of rock mass strength. *International Journal of Rock Mechanics and Mining Sciences*. 34: 1165-1186.
- [4]. Goodman, R. (1989). Introduction to rock mechanics. John Wiley and Sons. New York. United States.
- [5]. Goodman, R. and Shi, G.H. (1985). Block theory and its applications to rock engineering. Prentice-Hall, INC. New Jersey.
- [6]. Jaeger, J.C. and Cook, N.G.W. (1979). Fundamental of rock mechanics. 3th Edition. Chapman and Hall.
- [7]. Hallbauer, D.K., Wagner, H. and Cook, N.G.W. (1973). Some observations concerning the microscopic and mechanical behaviour of quartzite spacemen in stiff, triaxial compression test. *Int. J. Rock Mech.* 10: 713-726.
- [8]. Zoorabadi, M. and Gale, W. (2017). Review of roof support options for next generation of continuous miner. ACARP project number of C25003.
- [9]. SCT Operations Pty Ltd. (2000). Training manual on coal mine rock mechanics properties.
- [10]. Shen, J., Karakus, M. and Xu, C. (2012). A comparative study for empirical equations in estimating deformation modulus of rock masses. *Tunnelling and underground space technology*. 32: 245-250.
- [11]. Zoorabadi, M. (2010). Investigating intact rock strength and rock mass environment effects on rock mass deformation modulus using sensitivity analysis of empirical equations. In *Proceeding of Eurock 2010*. Lausanne Switzerland. Taylor and Francis Group. pp. 189-192.
- [12]. Zoorabadi, M. (2016). Deformability modulus of jointed rocks, limitation of empirical methods, and introducing a new analytical approach. Coal Operations conference. Wollongong. Australia.
- [13]. Brown, E.T. (1978). Trend in relationship between measured rock in situ stresses and depth. *International Journal of Rock Mechanics and Mining Science & Geomechanics*. 15: 211-215.
- [14]. Nemcik, J., Gale, E. and Mills, K. (2005). Statistical analysis of underground stress measurements in Australian coal mines. Bowen Basin Symposium. Yeppoon. Qld. Australia.
- [15]. Savage, W.Z., Swolfs, H.S. and Amadei, B. (1992). On the state of stress in the near-surface of the Earth's crust. *Pure Appl. Geophys.* 138: 207-228.
- [16]. Gale, W. and Blackwood, R.L. (1986). Three dimensional computational modelling of stress and rock failure distributions about the face of a rectangular underground opening and its correlation with coal mine roadway behaviour. *Int. J. Rock. Mech. And Mining Sci.*
- [17]. Zoorabadi, M. and Rajabi, M. (2017). Impact of bedding plane and laminations on softening zone around the roadways- 3D numerical assessment. Coal Operation Conference. Wollongong. Australia.
- [18]. Gale, W. (2013). Update of stress concentration effects about longwall panels for improved mine planning, ACARP project number of C20031.

مدل سازی عددی راهروهای معادن زغال سنگ - عدم قطعیت ناشی از استفاده روش های تجربی برای تخمین پارامترهای ورودی و تنش های برجا

مهدی زورآبادی^{۱،۲}

۱- مهندس ارشد ژئوتکنیک، شرکت SCT Operations Pty Ltd، ولونگونگ، استرالیا

۲- بخش مهندسی معدن، دانشگاه نیوساوت ولز، سیدنی، استرالیا

ارسال ۲۰۱۷/۱/۱۲، پذیرش ۲۰۱۷/۶/۱۲

نویسنده مسئول مکاتبات: m.zoorabadi@sct.gs; m.zoorabadi@unsw.edu.au

چکیده:

مدل سازی عددی یکی از روش های رایج برای تحلیل پایداری راهروها و فضاهای زیرزمینی، سطوح شیب دار و تخمین نشست زمین در پروژه های مهندسی معدن و عمران است. علیرغم پیشرفت های چشمگیر در روش های عددی و توسعه سخت افزارهای با سرعت پردازش بالا، مدل های رفتاری سنگ و پارامترهای ورودی مدل همچنان اصلی ترین عوامل بروز خطا در مدل سازی عددی هستند. این مسئله با رایج شدن استفاده از روش های تجربی برای تخمین پارامترهای ورودی مدل عمیق تر هم شده است. کاربران مدل های عددی بدون توجه به مکانیسم واقعی شکست و تغییر شکل سنگ، از روش های تجربی برای تعیین پارامترهای ورودی مدل های خود استفاده می کنند. برای مثال رایج ترین روش های تجربی، مقدار ثابتی را برای مدول تغییر شکل پذیری سنگ در همه عمق ها محاسبه می کنند که کاملاً مغایر رفتار واقعی سنگ است. مدول تغییر شکل پذیری سنگ یک پارامتر وابسته به تنش بوده و با تغییر عمق تغییر می کند. علاوه بر این، مکانیسم واقعی شکست و تغییر شکل سنگ با تغییر شکل یک مدول پیوسته که در اکثر روش های عددی فرض می شود متفاوت است. جدای از پارامترهای مقاومتی و تغییر شکل پذیری سنگ، بزرگای و جهت تنش های برجا هم پارامترهای مهمی هستند که تأثیر آن ها در مدل سازی رایج عددی در نظر گرفته نمی شوند. در این پژوهش، تأثیر استفاده بی رویه از روش های تجربی تخمین پارامترهای ورودی بر عدم قطعیت نتایج حاصل از مدل سازی عددی فضاهای زیرزمینی مورد بحث قرار داده شده است. همچنین تأثیر بزرگای و جهت تنش های برجا بر شکست سنگ ناشی از تنش در اطراف فضاهای زیرزمینی ارزیابی شده است.

کلمات کلیدی: مدل سازی عددی، شکست سنگ، روش های تجربی، تنش های برجا.
